Reduction in Barreling of Hollow Cylinder by Combination of Axial Compression and Circumferential Torsion in Upsetting with Conical Dies

Ryo Matsumoto[1*], Sotaro Tanaka[1] and Hiroshi Utsunomiya[1]

[1] Division of Materials and Manufacturing Science, Osaka University, Osaka, Japan
*ryo@mat.eng.osaka-u.ac.jp

Abstract. To reduce barreling of hollow cylinder in upsetting, circumferential one-way torsion with twist/compression speed of 0–12 °/mm was combined with axial compression in upsetting. Due to combination of compression and torsion, the plastic flow of the workpiece was enhanced in the outer radial direction on the die–workpiece interface. Barreling was reduced by combining compression and torsion with lower than 5 °/mm, whereas hourglass deformation occurred by combining compression and torsion with higher than 6 °/mm. The workpiece was successfully deformed without barreling and hourglass deformation (0.97 < fraction of diameters of height center/end face < 1.01) by interrupting the die rotation in upsetting with reduction in height of lower than 50%.

Keywords: Forging, Torsion, Stress superposition, Plastic flow, Hollow cylinder, Barreling.

1 Introduction

Due to strong demand on lightweight structural component of vehicles, forming process of hollow component is one of crucial technical targets. Shape defects of the components such as barreling, bending and plastic buckling easily occur in forming of hollow components because plastic deformation of hollow component is sensitive to nonuniform, local deformations and plastic instability. Major conventional solution to prevent such shape defects is the lubrication between the die and the components during forming [1]. In other solutions, pulsation of oil pressure to reduce plastic buckling and fracture in hydroforming of tubes [2] and filling hollow part with oil to expand in radial direction in ring compression [3] have been proposed. Axial compressive load and plastic flow of hollow components are controlled in these solutions.

A well-known approach to control axial load and plastic flow is combination of axial compression and circumferential torsion in axisymmetrical forming process. Theoretical analysis of the superposition of axial and shear stresses has been reported on changes in stress and strain components [4]. The applications of stress superposition in metal forming processes have been reviewed [5]. Especially KOBO type forming

process [6] is a well-established forging process with torsion to reduce axial forming load and refine the grain of the workpiece. The authors also investigated the reduction of axial forming load [7] and the microstructure evolution [8] in upsetting with torsional oscillation. On the other hand, the application of the change in plastic flow direction by the stress superposition is not sufficiently reported. It is supposed that the plastic flow in the lateral direction is assisted by combining axial deformation with circumferential torsion. The authors reported the enhancement of plastic flow in the lateral direction in lateral extrusion with torsional oscillation [9]. The enhancement of plastic flow in the lateral direction is expected to be applied to reduce the barreling in upsetting of hollow cylinder.

In order to reduce barreling of hollow cylinder in upsetting, circumferential torsion is combined with axial compression during upsetting in this study. The influence of one-way torsion on plastic flow of the hollow cylinder is investigated in upsetting with conical dies by the experiment and the finite element analysis.

2 Experimental Conditions

Fig. 1 shows the schematic illustration of upsetting with one-way torsion. The cylindrical workpiece was allocated between the dies with conical end surface aligning the center axes of the workpiece and the dies in the z direction (axial direction). The workpiece was simultaneously compressed in the z direction and twisted with one-way in the θ direction (circumferential direction) with respect to the compression axis. The dimensions of the initial workpiece were D_0 = 10.0 mm in outer diameter, d_0 = 5.0 mm in inner diameter and h_0 = 15.0 mm in height, while the apex angle of the end surface of the die was 160°. JIS A1070 aluminum was used as the workpiece material, while JIS SKH51 high-speed tool steel (63 HRC) was used as the die material. The end surfaces of the workpiece were machined to be Ra = 0.30–0.50 μm in arithmetic mean roughness, while the end surface of the dies was polished to mirror-like finish (Ra = 0.02–0.03 μm).

Upsetting was conducted without lubrication at room temperature. The axial compression speed of the upper ram was set to v = 0.1 mm/s, while rotation speed of the lower ram was set to ω = 0–0.5 rpm (0–0.05 rad/s). The lower ram started to rotate when the axial compression load reached 5 kN (reduction in height: approximately 5%). Here the reduction in height was defined as follows.

$$\Delta h/h_0 = (h_0 - h_{max})/h_0 \quad (1)$$

where h_{max} was the height of the outer corner of the compressed workpiece. The workpiece was twisted in one-way direction by frictional force between the die and the workpiece.

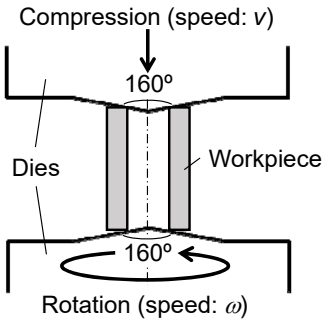

Fig. 1. Schematic illustration of upsetting with one-way torsion for hollow cylindrical workpiece using conical dies.

3 Finite Element Analysis Conditions

In parallel with the forging experiments, the finite element analysis was carried out by using a commercial three-dimensional finite element code, Simufact Forming ver. 15.0 (MSC Software Company). In the analysis, the elastic-plastic finite element method for deformation and the heat conduction finite element method for temperature change were applied to calculate the stress, strain, and temperature of the workpiece.

The workpiece was assumed to be a pure aluminum for industrial use, while the dies were treated as rigid bodies with isothermal state. The material properties of the aluminum workpiece were employed from the built-in database of material properties in Simufact Forming ver. 15.0. The frictional condition on the die–workpiece interface was assumed to be coefficient of friction $\mu = 0.1$. The coefficient of friction was determined to be agreed with the twisted angle of the workpiece in the experiment and the finite element analysis under various coefficients of friction. The heat transfer coefficients on the die–workpiece interface and the free surfaces of the workpiece were assumed to be 5000 W/(m^2·K) and 50 W/(m^2·K), respectively. Above analysis conditions were described in detail in our previous reports on upsetting with torsional oscillation [7,9].

4 Experimental Results

4.1 Axial Load and Torque

Fig. 2 shows the experimental results of the axial load and the torque. The workpiece was circumferentially twisted by means of the circumferential rotation of the lower die because the torque increased immediately after the die rotation started at $\Delta h/h_0 = 5\%$. Due to superposition of the axial compression and torsion stresses, the axial load was reduced by 10–20% with the torque increased.

The twisted angle of the workpiece in the one-way torsion was plotted in Fig. 3. Here the twisted angle of the workpiece was estimated by the circumferential angle between the two lines scribed on the upper and lower end surfaces of the workpiece. The twisted angle the workpiece increased almost linearly with reduction in height, however the twisted angle of the workpiece was much lower than the rotation angle of the lower die. This is because the circumferential slip occurred on the die–workpiece interface. The twisted speed (ω_t) estimated from the twisted angle and die rotation duration was approximately 0.08, 0.1 and 0.2 rpm in $\omega = 0.1$, 0.3 and 0.5 rpm, respectively. The axial load was reduced by approximately 14% with $\omega_t = 0.3$ rpm in upsetting with grooved dies [7]. Hence 10–20% reduction in axial load in Fig. 2 is reasonable for the torsion with $\omega = 0.5$ rpm ($\omega_t = 0.2$ rpm).

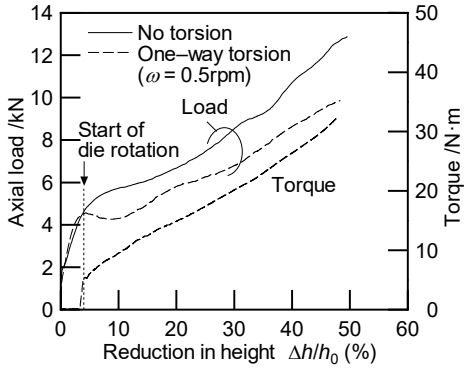

Fig. 2. Axial load and torque in upsetting of hollow cylinder.

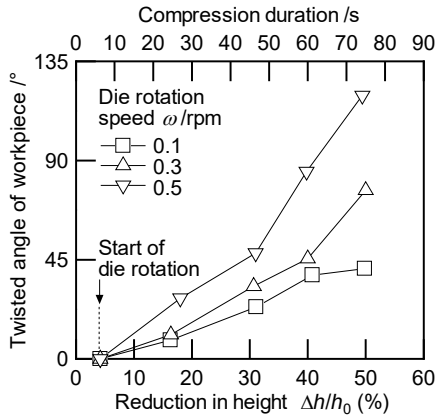

Fig. 3. Twisted angle of hollow cylinder during upsetting with torsion estimated from scribed lines on surfaces of hollow cylinder.

4.2 Deformation of Workpiece

Fig. 4 shows the photographs of the rz cross-section of the hollow cylinder after upsetting with conical dies. Here some surface scratches on the inner surface of the workpiece are due to machining scratches for the initial workpiece. The wall thickness of the workpiece was 1.2–1.4 times thicker than that of the initial workpiece in upsetting with/without torsion at $\Delta h/h_0 = 40\%$. Barreling ($D_c/D_e > 1.0$, $d_c/d_e > 1.0$) occurred in upsetting with $\omega = 0$ rpm, whereas hourglass deformation ($D_c/D_e < 1.0$, $d_c/d_e < 1.0$) occurred in upsetting with $\omega = 0.3$ and 0.5 rpm ($\omega_t/v = 6$ and 12 °/mm). Here the subscripts *c* and *e* for the diameters identify height center and end face (top, bottom) of the workpiece, respectively.

The measurement results of the outer and inner diameters of the hollow cylinder after upsetting are shown in Fig. 5. D_c/D_e and d_c/d_e increased to larger than 1.1 in upsetting with $\omega = 0$ rpm at $\Delta h/h_0 > 15\%$, whereas D_c/D_e and d_c/d_e decreased to 0.70–0.98 in upsetting with $\omega = 0.5$ rpm ($\omega_t/v = 12$ °/mm) at $\Delta h/h_0 > 30\%$. Due to increase of die rotation speed, the circumferential sliding of the workpiece increased in the outer radial direction on the die–workpiece contact by the die rotation.

To examine the influence of the die rotation mode on the deformation of the workpiece, following two rotation modes of the lower die were demonstrated in upsetting of the hollow cylinder.

(a) Start of die rotation at $\Delta h/h_0 = 30\%$ ($\omega = 0.5$ rpm at $\Delta h/h_0 > 30\%$)

(b) Stop of die rotation at $\Delta h/h_0 = 30\%$ ($\omega = 0.5$ rpm at $\Delta h/h_0 < 30\%$, no rotation at $\Delta h/h_0 > 30\%$)

The measurement results of the deformation behavior of the workpiece (D_c/D_e, d_c/d_e) are shown as the dashed line in Fig. 5. D_c/D_e and d_c/d_e decreased just after start of the die rotation in upsetting with die rotation mode (a), whereas they increased just after stop of the die rotation in upsetting with die rotation mode (b).

From above results, the superposition of circumferential torsion and axial compression is effective to control barreling and hourglass deformation of the hollow cylinder.

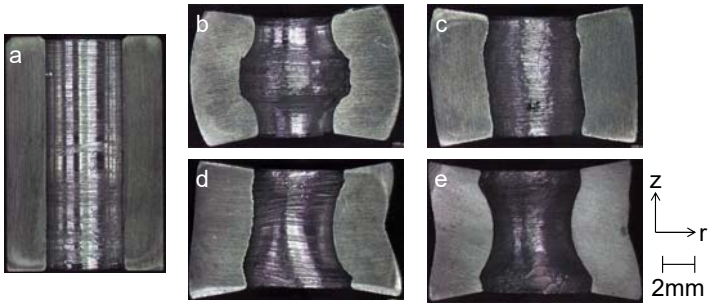

Fig. 4. Photographs of rz cross-section of hollow cylinder after upsetting with conical dies under several die rotation speeds ($\Delta h/h_0 = 40\%$). a: initial ($\Delta h/h_0 = 0\%$), b: $\omega = 0$ rpm (no torsion), c: $\omega = 0.1$ rpm, d: $\omega = 0.3$ rpm, e: $\omega = 0.5$ rpm.

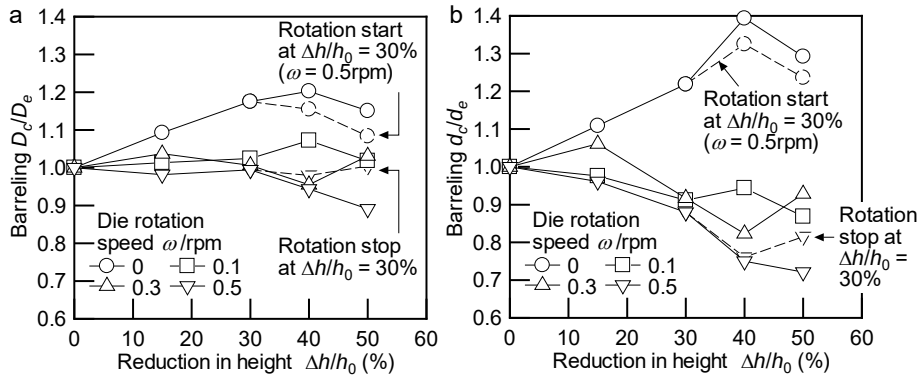

Fig. 5. Experimental results of barreling of hollow cylinder in upsetting with conical dies under several die rotation speeds (subscript *c*: height center, *e*: end face (top, bottom)). a: outer diameter, b: inner diameter.

5 Discussions by Finite Element Analysis

5.1 Radial Velocity and Plastic Flow of Workpiece

Fig. 6 shows the twisted angle of the hollow cylinder between the experimental results and the finite element analysis results in upsetting with torsion. The good agreement of the twisted angle between the experiment and the finite element analysis was confirmed. Therefore the material properties of the workpiece and the boundary conditions of the die–workpiece interface, especially the frictional condition in the finite element analysis were proper.

Fig. 7 shows the finite element analysis results of the radial velocity in the rz section of the hollow cylinder in upsetting with torsion. In upsetting with $\omega = 0$ rpm, the radial velocity at the height center was higher than the radial velocity at the top and bottom ends. This is due to the geometrical shape of the die and the friction at the die–workpiece interface. On the other hand, the radial velocity at the top and bottom ends increased with increasing rotation speed, whereas the radial velocity at the height center decreased. The increase of the radial velocity leads to enhance the plastic flow in the outer radial direction. From the velocity distribution in upsetting with torsion, the plastic flow in the outer radial direction at the top and bottom ends was indicated to be larger than that at the height center. As the results, barreling occurred in upsetting with $\omega = 0$ rpm, whereas hourglass deformation occurred in upsetting with $\omega \geq$ 0.3 rpm.

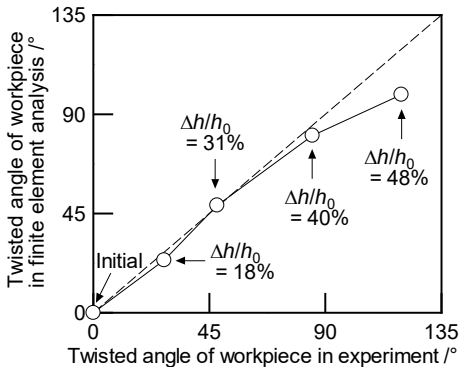

Fig. 6. Comparison of twisted angle of hollow cylinder between experimental results and finite element analysis results in upsetting with torsion ($\omega = 0.5$ rpm).

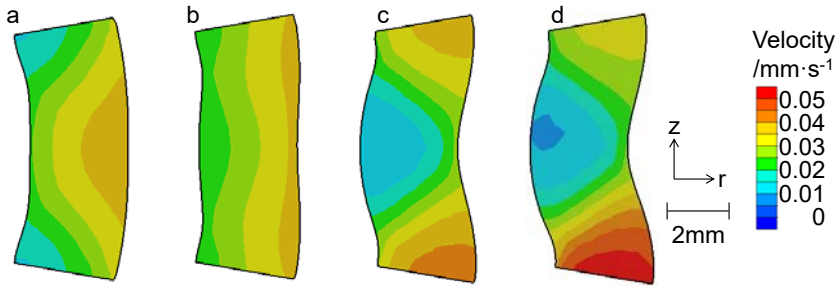

Fig. 7. Finite element analysis results of distribution of radial velocity in rz cross-section (right half) of hollow cylinder in upsetting with torsion ($\Delta h/h_0 = 50\%$). a: $\omega = 0$ rpm (no torsion), b: $\omega = 0.1$ rpm, c: $\omega = 0.3$ rpm, d: $\omega = 0.5$ rpm.

5.2 Control of Barreling Deformation

To attain to the deformation with $0.99 < D_c/D_e < 1.01$ (no barreling and no hourglass deformation) in upsetting of the hollow cylinder at $\Delta h/h_0 = 50\%$, the die rotation was controlled sequentially. The die started to be rotated with $\omega = 0.5$ rpm at $\Delta h/h_0 = 5\%$. When the workpiece was deformed to $D_c/D_e < 1.00$, the die rotation was temporally interrupted. On the other hand, when the workpiece was deformed to $D_c/D_e > 1.01$, the die rotation was restarted with $\omega = 0.5$ rpm.

Fig. 8 shows the finite element analysis results of D_c/D_e of the workpiece during upsetting. Since the end faces of the workpiece were deformed along the gradient of the end face of the die, D_c/D_e increased at $\Delta h/h_0 < 10\%$ in upsetting with/without die rotation. However, the workpiece was successfully deformed with $D_c/D_e = 1.00$ at $\Delta h/h_0 = 50\%$ by interrupting the die rotation twice at $19\% < \Delta h/h_0 < 28\%$ and $\Delta h/h_0 > 31\%$. Fig. 9 shows the finite element analysis results of the equivalent strain of the workpiece after upsetting with $\Delta h/h_0 = 50\%$. Barreling and hourglass deformation

were significantly reduced by the die rotation control, however double barreling occurred.

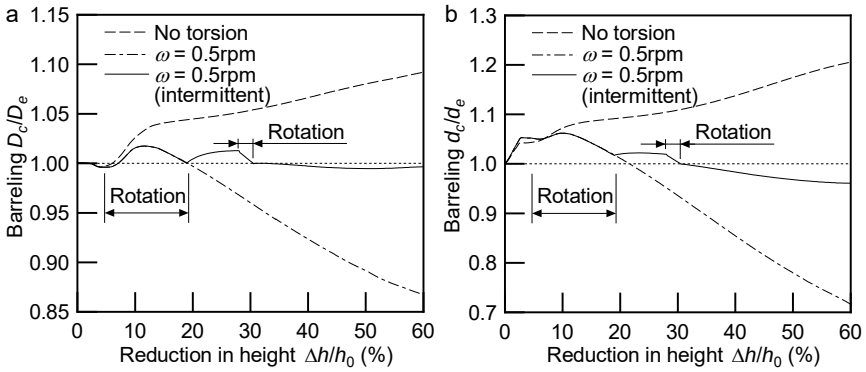

Fig. 8. Barreling of hollow cylinder in upsetting under controlling rotation of lower die (ω = 0.5 rpm, finite element analysis). a: outer diameter, b: inner diameter.

Die rotation speed ω /rpm	0	0.5	0.5 (intermittent)			
Equivalent strain	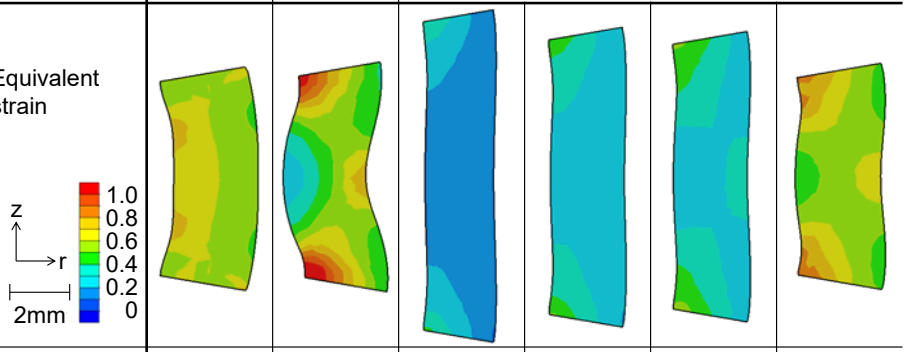					
$\Delta h/h_0$ (%)	50	50	19 (stop of die rotation)	28 (restart of die rotation)	31 (stop of die rotation)	50
D_c/D_e	1.08	0.89	1.00	1.01	1.00	1.00
D_{max}/D_{min}	1.08	1.15	1.02	1.03	1.02	1.03
d_c/d_e	1.17	0.78	1.02	1.02	1.00	0.97
d_{max}/d_{min}	1.18	1.31	1.05	1.06	1.05	1.08

Fig. 9. Finite element analysis results of distribution of equivalent strain in rz cross-section (right half) of hollow cylinder during upsetting under controlling rotation of lower die (D_{max}: maximum outer diameter, D_{min}: minimum outer diameter, d_{max}: maximum inner diameter, d_{min}: minimum inner diameter).

6 Conclusions

In this study, the influence of circumferential torsion on plastic flow of hollow cylinder was investigated in upsetting with conical dies. The workpiece was simultaneously compressed and twisted with one-way with respect to the compression axis by the frictional force between the die and the workpiece. Barreling was reduced by combining compression and torsion with twist/compression speed of lower than 5 °/mm, whereas hourglass deformation occurred by combining compression and torsion with higher than 6 °/mm. The workpiece was successfully deformed without barreling and hourglass deformation (0.97 < fraction of diameters of height center/end face < 1.01) by interrupting the die rotation in upsetting with reduction in height of lower than 50%.

Acknowledgement

This study was financially supported in part by the Amada Foundation (AF-2019007-B2).

References

1. Osakada K, Mori K (1986) A study of buckling in upsetting by use of finite element method. CIRP Annals – Manufacturing Technology 35(1):161–164.
2. Mori K, Maeno T, Maki S (2007) Mechanism of improvement of formability in pulsating hydroforming of tubes. International Journal of Machine Tools and Manufacture 47(6):978–984.
3. Tatematsu Y, Morimoto M, Kitamura K (2018) Experiment and FE analysis of compression of thick ring filled with oil. Key Engineering Materials 767:141–148.
4. Bridgman PW (1943) On torsion combined with compression. Journal of Applied Physics 14:273–283.
5. Tekkaya AE, Becker C, Ortelt T, Grzancic G (2015) Utilizing stress superposition in metal forming. Proceedings of the 7th JSTP International Seminar on Precision Forging, pp. 1–6.
6. Bochniak W, Korbel A (2003) KOBO Type Forming: forging of metals under complex conditions of the process. Journal of Materials Processing Technology 134(1):120–134.
7. Matsumoto R, Kou J, Utsunomiya H (2017) Reduction in axial forging load by low-frequency torsional oscillation in cold upsetting. International Journal of Advanced Manufacturing Technology 93(1-4):933–943.
8. Ohnishi H, Takamoto K, Matsumoto H, Matsumoto R (2020) Microstructural evolution of a Ti-6Al-4V alloy produced by forging process combined with torsional motion. Journal of Manufacturing Processes 58:1161–1170.
9. Matsumoto R, Tanaka S, Utsunomiya H (2022) Enhancement of plastic flow in lateral direction by torsional oscillation in upsetting and lateral extrusion. Journal of Materials Processing Technology 299:117369.